Journal of Solid State Chemistry **159,** 46–50 (2001)
doi:10.1006/jssc.2001.9128, available online at http://www.idealibrary.com on IDEAL®

Neutron Diffraction, Mössbauer Spectrum, and Magnetic Behavior of $Ag_2FeMn_2(PO_4)_3$ with Alluaudite-like Structure

N. Chouaibi,*,† A. Daidouh,* C. Pico,*,[1] A. Santrich,‡ and M. L. Veiga*

*Departamento de Química Inorgánica I, Facultad de Ciencias Químicas, Universidad Complutense de Madrid, 28040 Madrid, Spain;
†Département de Chimie, Faculté des Sciences de Tetouan, Université Abdelmalek Essaidi, Tetouan, Morocco; and
‡Instituto de Ciencias de Materiales, CSIC, Cantoblanco, E-28049 Madrid, Spain

Received September 7, 2000; in revised form January 31, 2001; accepted February 15, 2001; published online May 4, 2001

The new compound $Ag_2FeMn_2(PO_4)_3$ has been synthesized using solid state reactions, and characterized by X-ray and neutron diffraction. It crystallizes in the monoclinic space group $C2/c$ with the parameters $a = 12.1466(3)$ Å, $b = 12.7328(4)$ Å, $c = 6.4999(5)$ Å, and $\beta = 114.53(3)^\circ$. Its structure is formed by $[FeMn_2O_{12}]_\infty$ chains of edge-sharing FeO_6 and MnO_6 octahedra. The chains are interconnected by the PO_4 tetrahedra giving rise to layers parallel to the *ac* plane and exhibiting a three-dimensional channel-like structure where the silver cations are located. The distribution of the FeO_6 and MnO_6 octahedra along the chains was determined by the neutron refinements. The Mössbauer spectral parameters indicate the presence of only Fe(III) octahedral sites. The reciprocal susceptibility variation shows a deviation from the Curie–Weiss law below 19 K, which can be attributed to a weakly ferromagnetic component owing to probable canting of antiferromagnetically coupled spins along the $[FeMn_2O_{12}]_\infty$ chains.

INTRODUCTION

The alluaudite-type structure, that was found for natural minerals, was reported first by Fisher in 1955 (1). Further, a great number of synthetic materials possessing this structure have been reported as a result of introducing different metal cations with different oxidation states (2–6). Such a structure, which is usually formulated as $AA'M'M_2(XO_4)_3$, contains the $[M_2(XO_4)_3]$ framework, that is also found in some other common structure types as garnet, nasicon, langbeinite, and $Sc_2(WO_4)_3$ (7, 8). The arrangement of the polyhedra in this framework (i.e., the way in which they are interconnected and distributed along the host lattice) leads to various symmetry types. In fact, the arrangement of the $[M_2(XO_4)_3]$ is cubic or nearly cubic-centered in garnet, nasicon, and $Sc_2(WO_4)_3$ (9) but is monoclinic or orthorhombic in alluaudite and langbeinite (10). Furthermore, some compounds can adopt two different structures simply on the basis of the temperature at which they are synthesized or upon changing one metal type (11, 12). For example, $NaCa_2Mg_2(AsO_4)_3$ adopts a garnet-type structure at low temperature (1123 K) and an alluaudite-type at high temperature (1223 K) (13).

The structure of the title compound consists of a $[FeMn_2(PO_4)_3]^{2-}$ framework, that is built up by chains of edge-sharing MnO_6–MnO_6–FeO_6 octahedra, running along the [101] direction. The chains are linked together via the common corners of phosphate tetrahedra to form sheets parallel to the *ab* plane. The projection of one sheet along [001] is shown in Fig. 1. Adjacent sheets are also connected through PO_4 tetrahedra (upper corners, Fig. 1) and the constituents are related by a 2_1-screw axis, parallel to the *b*-axis, thus giving rise to an open framework with two different kinds of channels running along the *c*-axis. The channels are occupied by the silver cations within an eight-fold coordination (14, 15) which suggest an ionic mobility in the compound.

This paper deals with the X-ray and neutron structure refinement, the Mössbauer study, and the magnetic behavior of the new $Ag_2FeMn_2(PO_4)_3$ compound.

EXPERIMENTAL

Synthesis

Powder samples of composition $Ag_2FeMn_2(PO_4)_3$ were prepared by solid state reactions methods, starting from $AgNO_3$, $Fe(NO_3)_3 \cdot 9H_2O$, $C_{10}H_{14}MnO_4$, and $(NH_4)_2HPO_4$ weighed in stochiometric quantities. The starting reactants were well mixed, ground in an agate mortar, and heated at 723 K for a time sufficient to cause evolution of gaseous substances (NO_x, H_2O, NH_3, CO_2). The product was then progressively calcined between 873 and 1173 K with intervening by mixing and grinding until no change was detected by X-ray diffraction.

[1] To whom correspondence should be addressed. E-mail: cpico@eucmax.sim.ucm.es.

0022-4596/01 $35.00

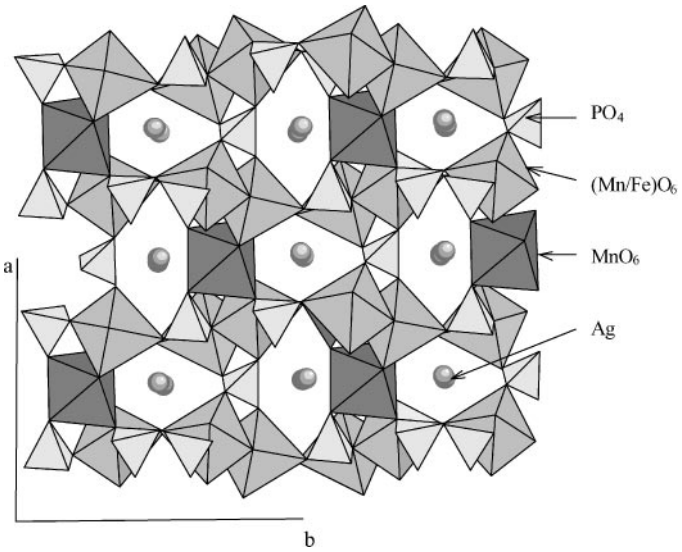

FIG. 1. Projection view along the [001] direction of the structure of $Ag_2FeMn_2(PO_4)_3$.

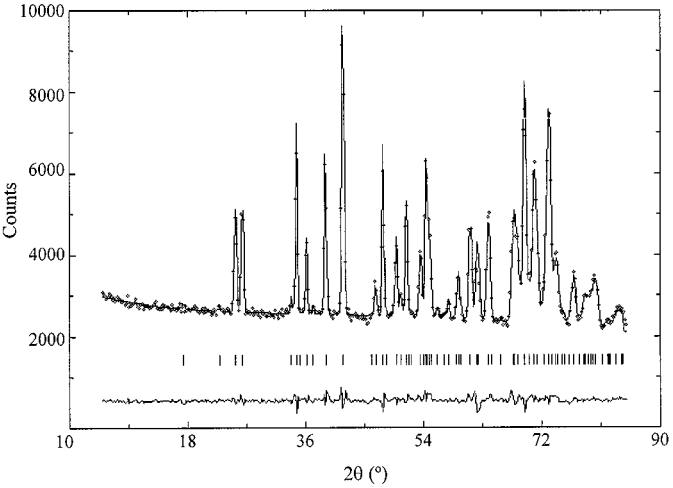

FIG. 3. Observed (crosses), calculated (solid line), and difference (bottom) time-of-flight neutron diffraction patterns of $Ag_2FeMn_2(PO_4)_3$ obtained from Rietveld refinements.

X-Ray and Neutron Diffraction

X-ray powder diffraction patterns were registered using a Philips X'Pert MPD diffractometer, Cu$K\alpha$ (1.5406 Å) radiation, a step scan of 0.04° (2θ) between 10 and 100° (2θ), and fixed-time counting of 12 s for each step. Neutron powder diffraction data were recorded at room temperature on the D1A high-resolution powder diffractometer ($\lambda = 1.9110$ Å) at the Institute Laue-Langevin (Grenoble, France). Both neutron and X-ray patterns were analyzed by the Rietveld method (FULLPROF program (16)). A pseudo-Voigt function was elected to generate the lineshape of the diffraction peaks.

Mössbauer Spectroscopy

Mössbauer spectra were obtained with a conventional spectrometer, which works in a constant acceleration mode. The velocity and isomer shift scales were calibrated with α-iron metal (6 μm thickness) as the standard and the spectra were analyzed at room temperature using the NORMOS program (17).

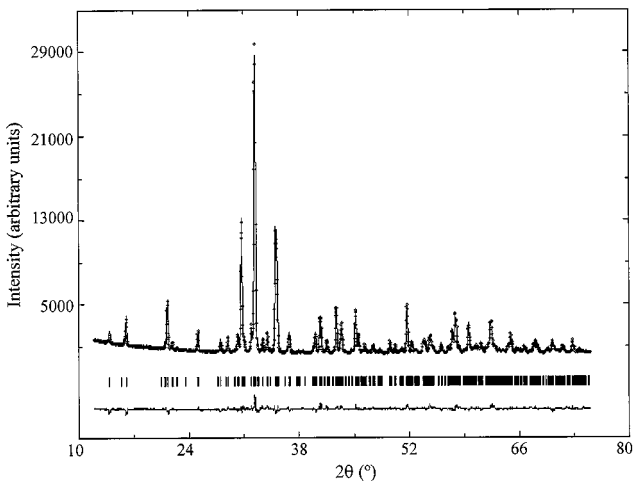

FIG. 2. Observed (crosses), calculated (solid line), and difference (bottom) X-ray powder diffraction patterns of $Ag_2FeMn_2(PO_4)_3$ obtained from Rietveld refinements.

TABLE 1
Crystallographic Data for $Ag_2FeMn_2(PO_4)_3$

1. Structure Parameters	
Crystal system	Monoclinic
Space group	$C2/c$
Unit cell dimensions	
a	12.1466(3) Å
b	12.7328(4) Å
c	6.4999(5) Å
β	114.5323(3)°
V	907.85(2) Å^3
Z	4
2. Structure Solution and Refinement	
R_P	9.2
R_W	9.1
R_B	3.1
R_F	2.8
χ^2	3.2
Refined parameters	46
Reflections	1360

TABLE 2
Atomic Coordinates of $Ag_2FeMn_2(PO_4)_3$

Atom	Position	x/a	y/b	z/c	$B_{eq} \times 10^2$ (Å)
Ag(1)	4*b*	0	$\frac{1}{2}$	0	2.720(5)
Ag(2)	4*e*	0	−0.0107(5)	$\frac{1}{4}$	2.032(5)
Mn	4*e*	0	0.2708(1)	$\frac{1}{4}$	1.590(5)
Fe/Mn	8*f*	0.2772(2)	0.6582(4)	0.3667(1)	1.896(3)
P(1)	4*e*	0	−0.2831(3)	$\frac{1}{4}$	0.012(5)
P(2)	8*f*	0.2357(5)	−0.1099(5)	0.1256(4)	0.481(1)
O(1)	8*f*	0.4554(4)	0.7133(4)	0.5331(1)	0.035(2)
O(2)	8*f*	0.0952(1)	0.6427(5)	0.2396(5)	1.132(3)
O(3)	8*f*	0.3306(4)	0.6658(3)	0.0995(5)	0.393(2)
O(4)	8*f*	0.1283(2)	0.4001(1)	0.3245(4)	0.301(2)
O(5)	8*f*	0.2226(5)	0.8226(4)	0.3166(5)	0.167(1)
O(6)	8*f*	0.3196(4)	0.4981(1)	0.3811(2)	0.713(3)

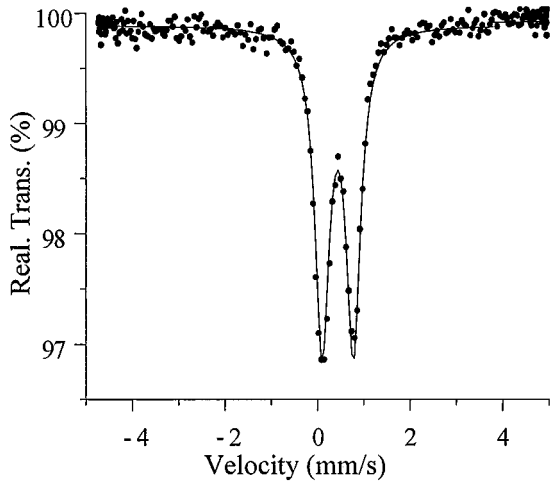

FIG. 4. Mössbauer spectrum of $Ag_2FeMn_2(PO_4)_3$ at room temperature.

Magnetic Measurements

Magnetic properties were performed with a Quantum design SQUID magnetometer. The temperature dependence of susceptibilities was registered at decreasing temperatures from 300 to 2 K at an applied field of 0.5 T. The field dependence of the magnetization was measured at 25, 10, and 2 K by varying the applied magnetic field between −60,000 and 60,000 G.

TABLE 3
Selected Bond Distances (Å) and Angles (deg) for $Ag_2FeMn_2(PO_4)_3$

Ag(1)–O(2)	2.360(1) × 2	Ag(2)–O(1)	2.881(3) × 2
Ag(1)–O(2)	3.020(5) × 2	Ag(2)–O(3)	2.928(4) × 2
Ag(1)–O(4)	2.400(4) × 2	Ag(2)–O(6)	2.661(5) × 2
Ag(1)–O(4)	2.612(2) × 2	Ag(2)–O(6)	2.492(2) × 2
Mn–O(1)	2.244(2) × 2	Fe–O(1)	2.099(4)
Mn–O(3)	2.303(4) × 2	Fe–O(2)	2.022(5)
Mn–O(4)	2.178(5) × 2	Fe–O(3)	2.092(3)
		Fe–O(5)	2.179(1)
P(1)–O(1)	1.561(1) × 2	Fe–O(5)	2.071(4)
P(1)–O(2)	1.515(3) × 2	Fe–O(6)	2.094(2)
P(2)–O(3)	1.522(5)	P(2)–O(5)	1.571(2)
P(2)–O(4)	1.549(4)	P(2)–O(6)	1.526(3)
O(1)–P1–O(1)	110.593	O(3)–P2–O(4)	72.614
O(1)–P1–O(2)	107.399	O(3)–P2–O(5)	72.736
O(1)–P1–O(2)	114.203	O(3)–P2–O(6)	110.003
O(2)–P1–O(2)	102.980	O(4)–P2–O(5)	109.221
		O(4)–P2–O(6)	110.512
		O(5)–P2–O(6)	109.095
O(1)–Mn–O(1)	141.996	O(1)–Fe/Mn–O(2)	164.057
O(1)–Mn–O(3)	71.472	O(1)–Fe/Mn–O(3)	78.649
O(1)–Mn–O(3)	86.550	O(1)–Fe/Mn–O(5)	86.573
O(1)–Mn–O(4)	117.232	O(1)–Fe/Mn–O(5)	82.718
O(1)–Mn–O(4)	91.976	O(1)–Fe/Mn–O(6)	96.905
O(3)–Mn–O(3)	109.046	O(2)–Fe/Mn–O(3)	109.184
O(3)–Mn–O(4)	85.056	O(2)–Fe/Mn–O(5)	79.601
O(4)–Mn–O(4)	81.840	O(2)–Fe/Mn–O(5)	88.122
O(3)–Mn–O(4)	164.425	O(2)–Fe/Mn–O(6)	97.508
		O(3)–Fe/Mn–O(5)	90.677
		O(3)–Fe/Mn–O(5)	161.059
		O(3)–Fe/Mn–O(6)	85.785
		O(5)–Fe/Mn–O(5)	84.810
		O(5)–Fe/Mn–O(6)	174.447
		O(5)–Fe/Mn–O(6)	99.894

RESULTS AND DISCUSSION

Structural Characterization

The structure of $Ag_2FeMn_2(PO_4)_3$ was first determined by X-ray powder diffraction. The corresponding refinement indices are $R_P = 13.7$, $R_{WP} = 15.2$, $R_B = 8.84$, and $R_F = 7.43$. The Rietveld refinement of the pattern yielded the monoclinic cell parameters $a = 12.145(1)$ Å, $b = 12.722(2)$ Å, $c = 6.497(1)$ Å, and $\beta = 114.52(3)^\circ$ taking

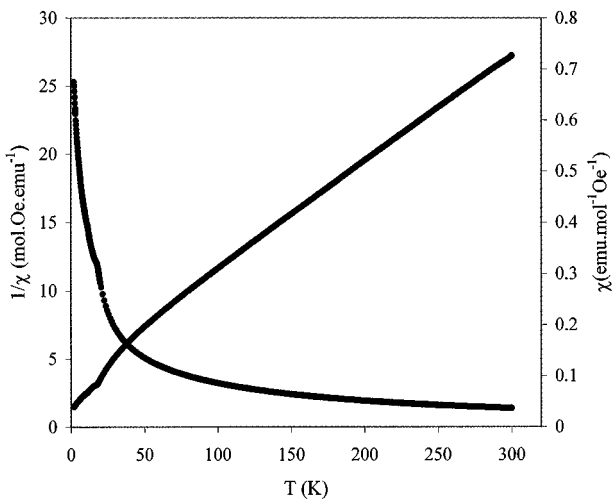

FIG. 5. Molar and inverse molar magnetic susceptibility data for $Ag_2FeMn_2(PO_4)_3$ in an applied filed of 500 G.

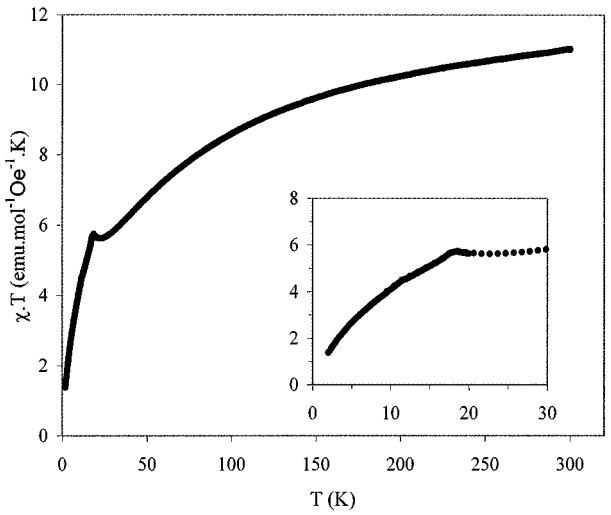

FIG. 6. Variation of the χT product versus temperature showing the magnetic transition phase at $T_N = 19$ K.

the structure of $NaCaCdMg_2(AsO_4)_3$ (2) as a trial model. The agreement with observed, calculated, and difference X-ray powder diffraction patterns is shown in Fig. 2.

For the neutron diffraction, the intensities of the reflections are somewhat different in comparison with those collected by X-ray powder experiments. The corresponding atomic coordinates obtained from the X-ray data were used as starting values for the Rietveld refinement of the neutron patterns, and the new results are shown in Fig. 3. The refinement yielded the parameters listed in Table 1 and the atomic positions in Table 2, from which the most representative bond lengths and angles have been calculated, as appear in Table 3.

The distribution of the transition metals (Fe, Mn) along the $[FeMn_2O_{12}]_\infty$ chains cannot be determined by using only X-ray diffraction refinements; i.e., there are two crystallographic positions available for these atos, 4*e* and 8*f*, because the X-ray scattering powers of Fe and Mn are nearly identical. In addition, Fe^{3+} and Mn^{2+} have the same number of electrons. Neutron diffraction results allowed to the refinement to be improved and the Fe and Mn atoms were fixed in the positions cited in Table 2. In fact, the mean values of the cation–oxygen distances for 4*e* and 8*f* positions (see Table 3) show that the 4*e* site is much larger than the 8*f* one, and it is likely that the larger position must be occupied by the bigger cation, Mn^{2+} in this case (ionic radius = 0.67 Å against 0.55 Å for Fe^{3+} cation in six-fold coordination (18).

Mössbauer Study

The Mössbauer spectrum of $Ag_2FeMn_2(PO_4)_3$, measured at room temperature, is shown in Fig. 4. The spectrum showed a unique asymmetric doublet corresponding to a nonordered magnetic phase, and the hyperfine parameters obtained from these experimental results were the isomer shift, $IS = 0.435(2)$ mm/s, and the quadruple splitting, $QS = 0.674(4)$ mm/s. The fits of the data show that iron is only present as a high-spin Fe^{3+} arrangement on octahedral sites, in accordance with the results obtained from the structural study.

Magnetic Behavior

The temperature dependence of the molar magnetic susceptibility data for $Ag_2FeMn_2(PO_4)_3$ cooled at zero field is illustrated in Fig. 5. The χ_M value increases with decreasing

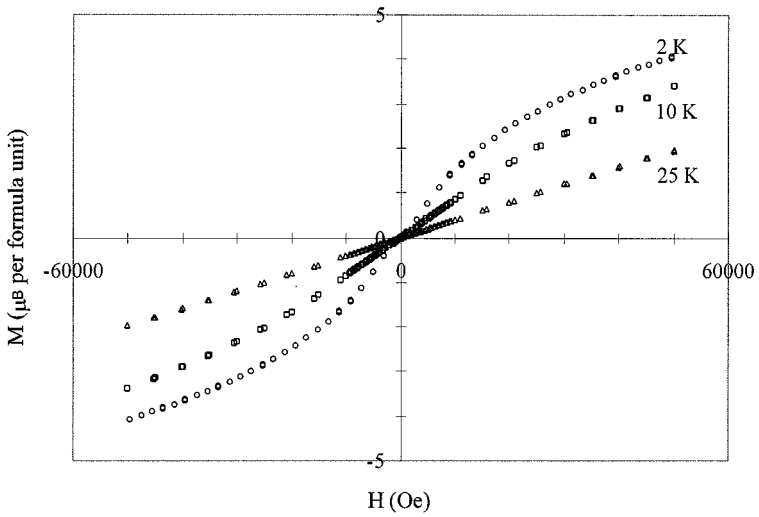

FIG. 7. Variation of magnetization with the magnetic field at 2, 10, and 25 K.

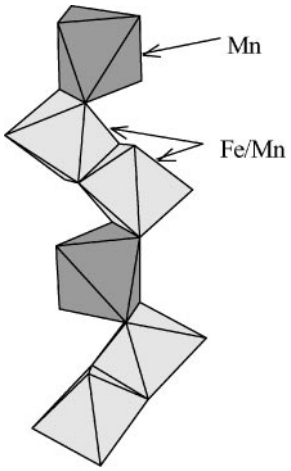

FIG. 8. Partial projection of the $[FeMn_2O_{12}]_\infty$ chains running along the [101] direction and showing the zigzag configuration.

temperatures in all the range of measurements. The variation of $1/\chi_M$ (Fig. 5) shows that the sample displays a Curie–Weiss law behavior between 19 to 300 K. A fit of the data to the Curie–Weiss equation $\chi_M = C/(T - \theta)$ yielded the following values of the constants: $C = 12.61\,\mathrm{g\,K\,mol^{-1}}$, $\theta = -45.52$ K. From the Curie constant, the paramagnetic moment for this material was $\mu = 10.04\,\mu_B$, which agrees well with the expected value of $10.25\,\mu_B$ for two Mn^{2+} cations and one Fe^{3+} cation in high-spin states.

The negative value of θ together with the continuous increase of χ_M with decreasing T indicate an antiferromagnetism behavior for this compound.

At low temperature, the inverse susceptibility data deviate from the Curie–Weiss linear variation and a slight increase is observed in the $\chi_M T$ versus temperature graph (Fig. 6) that reaches a maximum at 19 K. This fact can suggest the presence of a magnetic phase transition at the critical temperature $T_N = 19$ K.

The field dependence of magnetization carried out on this sample at different fixed temperatures is shown in Fig. 7. Above T_N (at 25 K) the straight line confirms the predominance of the paramagnetic behavior. However, below T_N (at 10 and 2 K), nonlinearity was clearly observed, suggesting the presence of a small ferromagnetic contribution. It appears that the antiferromagnetic spin alignment is disrupted, and such a behavior can be interpreted as a result of ferromagnetic canting or of a weak ferromagnetic contribution.

This magnetic behavior is similar to that observed in $KMn_4(PO_4)_3$ (19) and is very common in many phosphate and arsenate compounds (20–22). In fact, the antiferromagnetic spin coupling within the $[FeMn_2O_{12}]_\infty$ chains may be significantly weakened by the zig-zag configuration of the chains (Fig. 8) giving rise to nonlinear vector spins that lead to a weak ferromagnetic component appearing at low temperatures.

ACKNOWLEDGMENTS

We are indebted to the CICYT (MAT 2000-1585-C03-02) for financial support. We thank the ILL (Grenoble, France) for n.d. facilities and Dr J. Tornero for the Mössbauer data.

REFERENCES

1. D. J. Fisher, *Am. Mineral.* **40,** 1100 (1955).
2. D. Antenucci, A. M. Fransolet, G. Miehe, and P. Tarte, *Eur. J. Mineral.* **7,** 175 (1995).
3. M. B. Korzenski, G. L. Schimek, J. W. Kolis, and G. J. Long, *J. Solid State Chem.* **139,** 152 (1998).
4. K. H. Lii and J. Ye, *J. Solid State Chem.* **131,** 131 (1997).
5. F. Leroux, A. Mar, C. Payen, D. Guyomard, A. Verbaere, and Y. Piffard, *J. Solid State Chem.* **115,** 240 (1995).
6. T. E. Warner, W. Millius, and J. Maier, *J. Solid State Chem.* **106,** 301 (1993).
7. Y. Piffard, A. Verbaere, and M. Kinishita, *J. Solid State Chem.* **71,** 121 (1987).
8. E. R. Losilla, S. Bruque, M. A. G. Aranda, L. Moreno-Real, E. Morin, and M. Quarton, *Solid State Ionics* **112,** 53 (1998).
9. S. Oyetola, A. Verbaere, D. Guyomard, and Y. Piffard, *J. Solid State Chem.* **77,** 102 (1988).
10. A. Leclaire, A. Benmoussa, M. M. Borel, A. Grandin, and B. Raveau, *J. Solid State Chem.* **78,** 227 (1989).
11. S. Khorari, A. Rulmount, R. Cahay, and P. Tarte, *J. Solid State Chem.* **118,** 267 (1995).
12. S. Khorari, A. Rulmount, and P. Tarte, *J. Solid State Chem.* **134,** 31 (1997).
13. S. Khorari, A. Rulmount, and P. Tarte, *J. Solid State Chem.* **131,** 290 (1997).
14. A. Daidouh, M. L. Veiga, and C. Pico, *J. Solid State Chem.* **130,** 28 (1997).
15. A. Daidouh, M. L. Veiga, and C. Pico, *Solid State Ionics* **124,** 109 (1999).
16. J. Rodriguez-Carvajal, "Fullprof Program III," Grenoble, France, 1994.
17. R. A. Brand, *Nucl. Instrum. Methods Phys. Res. B* **28,** 398 (1987).
18. R. D. Shannon, *Acta Crystallogr., Sect. A* **32,** 751 (1976).
19. A. Daidouh, J. L. Martinez, M. L. Veiga, and C. Pico, *J. Solid State Chem.* **144,** 169 (1999).
20. J. P. Attifield, A. K. Cheetham, D. C. Jhonson, and C. C. Torardi, *Inorg. Chem.* **26,** 3379 (1987).
21. M. A. G. Aranda, S. Bruque, J. P. Attifield, F. Palacio, and R. B. V. Dreele, *J. Solid State Chem.* **132,** 202 (1997).
22. D. Papoutsakis, J. E. Jackson, and D. G. Nocera, *Inorg. Chem.* **35,** 800 (1996).